

## Beyond the Diffraction Limit and below 0.4 Angstroms with a High Dynamic Range Pixel Array Detector

Muller, D.<sup>1</sup>, Chen, Z.<sup>1</sup> and Jiang, Y.<sup>1</sup>

<sup>1</sup> Cornell University, United States

Advances in aberration-corrected electron optics have made sub-Angstrom resolution microscopy widely available. However, at the lower beam energies needed to avoid knock-on damage while imaging two-dimensional materials, the spatial resolution is limited to about one Angstrom from residual high-order geometric and chromatic aberrations. By phasing a series of scanning diffraction patterns, electron ptychography can in principle numerically retrieve the probe and object functions with a spatial resolution limited not by the numerical aperture of the lens, but by the largest scattering angle collected. To do so requires a detector that can record the full diffraction pattern - from central beam to high scattering angles, without saturation or distortion. This requires a dose rate, dynamic range and readout speed beyond that of conventional detectors.

Here, combining our new high-dynamic-range and single-electron-sensitivity electron microscope pixel array detector (EMPAD) [1] with full-field ptychography [2,3], we achieved a 0.4 Å resolution at 80 keV on an electron microscope which has  $\sim 1$  Å resolution limit with conventional STEM imaging methods. Figure 1 shows the annular dark field (ADF) image and ptychographic reconstructions of a monolayer MoS<sub>2</sub> using an EMPAD dataset taken with a 21.4 mrad semi-angle ( $\alpha$ ) probe. As shown in Figure 1(b)-(d), the reconstructed atoms become sharper as higher cutoff of the diffraction patterns is used. With the entire diffraction patterns (about  $4\alpha$  cutoff), the diffractogram of the reconstructed phase shown in Figure 1(h) reaches an information limit close to  $5\alpha$  - corresponding to a 0.39 Å Abbe resolution, while at the same dose and imaging conditions conventional ADF image is only  $2\alpha$ , *i.e.*, 0.98 Å Abbe resolution. Furthermore, the image contrast of the ptychographic reconstructions is significantly improved, showing a sulfur mono-vacancy defect that can be barely seen in the noisy ADF image.

For a real-space resolution test, we imaged a twisted bilayer of MoS<sub>2</sub> with twist angle  $\sim 6.8^\circ$ . This forms a Moiré pattern with a systematic range of separations between the projected atoms. The ptychographic reconstruction in Figure 2(b) shows many resolved atomic pairs that could not be resolved in the ADF image in Figure 2(a). Figure 2(c) shows an enlarged view of closely spaced atoms and the line profiles in Figure 2(d) show four selected peak-peak separations that approach resolution limit. The peak separation with  $0.42 \pm 0.02$  Å still contains a 6% dip at the middle point while more closely spaced atoms lose the central dip at just below 0.4 Å, which defines the Sparrow resolution limit, close to the Abbe resolution demonstrated in Figure 1(h).

### References:

[1] MW Tate, *et al*, Microscopy and Microanalysis **22** (2016), p. 237.

[2] A Maiden, *et al*, Ultramicroscopy 109 (2009), p. 1256.

[3] Y Jiang, *et al.*, arXiv: 1801.04630.

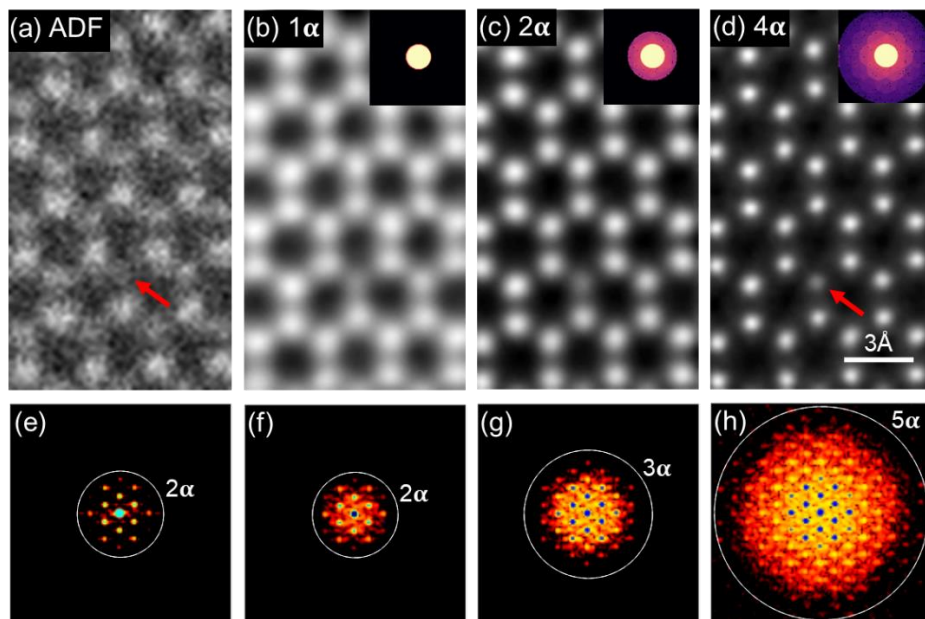


**Figure 1.** Resolution improvement of ptychographic reconstructions of monolayer  $\text{MoS}_2$  with increasing collection angle. (a) Synthesized ADF image from the same EMPAD dataset. Ptychographic reconstructions applying different cutoffs: (b) only the central bright field disk ( $1\alpha$ ), (c) up to  $2\alpha$ , and (d) up to  $4\alpha$ . (e)-(h) Diffraction patterns corresponding to (a)-(d) with white circles showing the information limit.  $5\Phi\#177$ ; corresponds to a  $0.39 \text{ \AA}$  Abbe resolution. The red arrows point out a sulfur mono-vacancy.

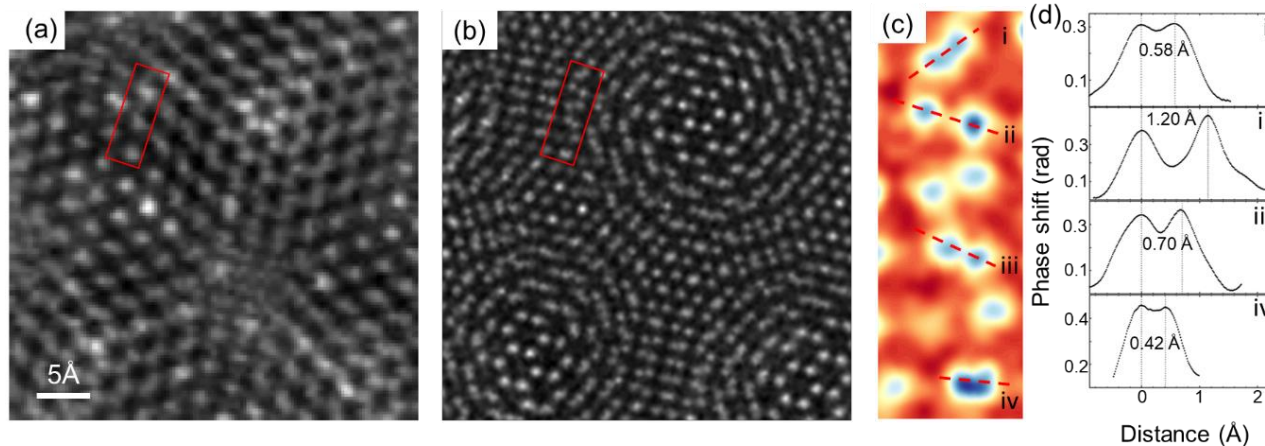


**Figure 2.** Real-space resolution demonstration of full-field ptychography using a twisted bilayer  $\text{MoS}_2$ . (a) Synthesized ADF image; (b) Phase image from ptychographic reconstruction of the same region as (a); (c) Enlarged phase image of the marked area in (b); (d) Line profiles of corresponding positions labeled with dashed red lines in (c). The peak separation distances are labelled in (d).

## Funding

Research supported by US National Science Foundation (grants DMR-1539918, DMR-1429155, DMR-1719875) & US Department of Energy Basic Energy Sciences (DE-SC0005827).